arXiv:1411.0788v1 [cond-mat.supr-con] 4 Nov 2014

# Fate of $yz/zx$ orbital degeneracy and $xy$ Fermi surface in Ru substituted $FeSe_{1-x}Te_x$

T. Sugimoto,[1] D. Ootsuki,[2] K. Sawada,[1] H. Anzai,[3] M. Arita,[3] H. Namatame,[3]
M. Taniguchi,[3,4] M. Horio,[5] K. Horiba,[6] M. Kobayashi,[6] K. Ono,[6] H.
Kumigashira,[6] T. Inabe,[7] T. Noji,[7] Y. Koike,[7] N. L. Saini,[8] and T. Mizokawa[1,2,8]

[1]*Department of Complexity Science and Engineering, University of Tokyo, 5-1-5 Kashiwanoha, Kashiwa 277-8561, Japan*
[2]*Department of Physics, University of Tokyo, 5-1-5 Kashiwanoha, Kashiwa 277-8561, Japan*
[3]*Hiroshima Synchrotron Radiation Center, Hiroshima University, Higashihiroshima, Hiroshima 739-0046, Japan*
[4]*Graduate School of Science, Hiroshima University, Higashihiroshima, Hiroshima 739-8526, Japan*
[5]*Department of Physics, University of Tokyo, 7-3-1 Hongo, Bunkyo-ku, Tokyo 113-0033, Japan*
[6]*Institute of Materials Structure Science, High Energy Accelerator Research Organization (KEK), Tsukuba 305-0801, Japan*
[7]*Department of Applied Physics, Tohoku University, Sendai 980-8579, Japan*
[8]*Dipartimento di Fisica, Universitá di Roma "La Sapienza", Piazzale Aldo Moro 2, Roma 00185, Italy*

(Dated: November 5, 2014)

We have investigated the impact of Ru substitution on the multi-band electronic structure of $FeSe_{1-x}Te_x$ by means of angle-resolved photoemission spectroscopy (ARPES). The ARPES results exhibit suppression of the $xy$ Fermi surface and the spectral broadening near the zone boundaries, which can be associated with the lattice disorder introduced by the Ru substitution. The degeneracy of the Fe 3$d$ $yz/zx$ bands at the zone center, which is broken in $FeSe_{1-x}Te_x$, is partly recovered with the Ru substitution, indicating coexistence of nematic and non-nematic electronic states.

PACS numbers: 74.25.Jb, 74.70.Xa, 79.60.-i, 74.81.-g

The discovery of high-$T_c$ superconductivity in Fe pnictides [1] has stimulated extensive experimental and theoretical investigations on the multi-orbital character of these. Among the Fe-based superconductors, $FeSe_{1-x}Te_x$ has the simplest crystal structure (anti-PbO type structure) with stacking of the FeSe(Te) layers and is thought to be the most suitable for the study of multi-orbital physics [2]. The electronic phase diagram of $FeSe_{1-x}Te_x$ is rich and very interesting due to spin and lattice instabilities that are probably related to the Fe 3$d$ multi-orbital character. One of the end members FeSe exhibits orthorhombic distortion below 90 K and superconductivity below 8 K [3]. The other end member FeTe becomes antiferromagnetic accompanied by orthorhombic lattice distortion [4]. $FeSe_{1-x}Te_x$ is basically tetragonal and exhibits superconductivity with a maximum $T_c$ $\sim$ 15 K [5]. Moreover, the charge neutral cleavage plane is an extra advantage to study multi-band Fermi surfaces of $FeSe_{1-x}Te_x$ using angle-resolved photoemission spectroscopy (ARPES). In spite of the apparent simplicity of the crystal structure of $FeSe_{1-x}Te_x$, the assignment of the orbital character in ARPES is still controversial. For example, out of the four hole bands observed near the zone center in ARPES, the outermost hole band (which is labeled as $\gamma$ in several literatures) forms the large Fermi pocket and is always very weak. This outermost hole band is assigned to $xy$ by Chen *et al.* using polarization dependent ARPES [6], consistent with most of the ARPES studies [7, 8], while Tamai *et al.* assign it to $yz/zx$ [9]. The intermediate hole band (labeled as $\beta$ in literatures) forms the small Fermi pocket and is assigned to $yz/zx$ [6] or $xy$ [10]. The inner most band that almost touches the Fermi level (labeled as $\alpha$ in literatures) is assigned to $yz/zx$ [6, 10]. In addition, Okazaki *et al.* [10] resolve another intermediate hole band which does not reach the Fermi level and is almost degenerate with the inner most hole band at the zone center. We will call this intermediate hole band as $\beta'$. The orbital degeneracy of $yz/zx$ bands ($\alpha$ and $\beta'$) at the $\Gamma$ point is likely to be confirmed by Okazaki *et al.* although it is not observed in most of the ARPES works. Another possibility is that the hole band assigned to $xy$ by Okazaki *et al.* (corresponding to $\beta$) is one of the $yz/zx$ bands and, instead, the inner most band assigned to $yz/zx$ by Okazaki *et al.* (corresponding to $\alpha$) would be $xy$ as proposed by Sudayama *et al.* [7]. With this orbital assignment, the orbital degeneracy of $yz/zx$ is actually removed even in the result by Okazaki *et al.* in which the $\beta$ and $\beta'$ are successfully resolved. Such a puzzling situation indicates complexity of the electronic states in $FeSe_{1-x}Te_x$ that has been overlooked in the interpretation of ARPES results.

Local structural studies have revealed that the Se and Te atoms are distributed with short Fe-Se bonds and long Fe-Te bonds [11]. The different bond length and chalcogen height between Fe-Se and Fe-Te indicate that the ligand field splitting between $xy$ and $yz/zx$ can be reversed between the elongated $FeTe_4$ and compressed $FeSe_4$ tetrahedron and that the $yz/zx$ orbital degeneracy can be removed in the $Fe(Se,Te)_4$ tetrahedron. If the $yz/zx$ orbital degeneracy is locally broken, then the band splitting between the $yz/zx$ bands at the $\Gamma$ point can be explained naturally. In addition, the crystal field reverse between $xy$ and $yz/zx$ can provide a possible explana-

tion of the two $xy$ (outer and inner) bands near Γ point as pointed out by Sudayama *et al.* [7]. In this context, since the electronic structure of $FeSe_{1-x}Te_x$ is complicated by the local symmetry breaking, more systematic investigations are required to understand the intervening coupling between the local disorder and the multi-orbital electronic states.

In order to address this issue, we focus on isovalent Ru substitution effect on the multi-band electronic structure of $FeSe_{1-x}Te_x$. It is known that the transition-metal impurity can enhance anisotropic transport in Fe pnictides [12, 13], and the origin of the anisotropy is assigned to anisotropic impurity scattering [14]. Therefore, it is highly important to study the transition-metal impurity effect on the multi-band electronic state by means of ARPES. In this paper, we report an ARPES study on Ru substituted $FeSe_{1-x}Te_x$ which reveals the impact of local symmetry breaking on the multi-band electronic structure of $FeSe_{1-x}Te_x$.

Single crystals of $Fe_{0.95}Ru_{0.05}Se_{0.3}Te_{0.7}$ were grown by the Bridgman method and annealed at 400 °C for 200 h in vacuum ($10^{-6}$ Torr) [5, 15]. The ARPES measurements at $h\nu$ = 23 eV were performed at beamline 9A, Hiroshima Synchrotron Radiation Center (HSRC) which has a normal incidence monochromator with off-plane Eagle mounting. Circularly polarized light from the helical undulator was exploited for the ARPES experiments. The photoelectrons were collected using a SCIENTA R4000 analyzer. Total energy resolution including the monochromator and the electron analyzer was set to 19.9 meV. The angular resolution was set to ∼ 0.2° that gives the momentum resolution of 0.0077 Å$^{-1}$ for $h\nu$ = 23 eV. The base pressure of the spectrometer was $10^{-9}$ Pa range. We cleaved the single crystals at 20 K under the ultrahigh vacuum and took ARPES data at the same temperature within four hours after the cleavage. The ARPES measurements for $h\nu$ = 37 to 56 eV were performed at beamline 28A of Photon Factory, KEK using a SCIENTA SES-2002 electron analyzer with circularly polarized light in order to avoid the relatively strict selection rule of the linear polarization and to observe various Fe 3$d$ orbital symmetries. The total energy resolution was set to 26.2 - 50.7 meV for $h\nu$ = 37 - 56 eV. The angular resolution was set to ∼ 0.2° that gives the momentum resolution of 0.010 - 0.013 Å$^{-1}$ for $h\nu$ =37 - 56 eV. The base pressure of the spectrometer was in the $10^{-9}$ Pa range. The spectra were acquired at 20 K within 12 hours after the cleaving. In all the ARPES measurements, the single crystals were properly oriented on the sample stage by the standard Laué measurements and were cooled using liquid He refrigerator. The Fermi level ($E_F$) was determined using the Fermi edge of gold reference samples.

Figures 1(a) and (b) show the photoemission intensity maps at $E_F$ with left- and right-handed circular polarization (LCP and RCP), respectively. The top of the $\alpha$ band (almost touching $E_F$) at the zone center and the $\beta$ Fermi surface are clearly observed. The butterfly-like shape of the $\beta$ Fermi surface, which is induced by the transition-matrix element effect, is rotated clockwise or counterclockwise depending on the helicity of the circularly polarized light. This indicates that the $\beta$ Fermi surface is derived from one of the Fe 3$d$ $yz/zx$ bands. The intense $\alpha$ band at the zone center should be assigned to the other Fe 3$d$ $yz/zx$ band since the suppression of the Fe 3$d$ $xy$ band is expected at the zone center due to the four-fold symmetry around the surface normal axis. The sum of the LCP and RCP maps is displayed in Figure 1(c) where the two Fermi surfaces are more clearly seen. Figures 1(d) and (e) show the photoemission intensity maps at 20 meV below $E_F$ with LCP and RCP, respectively. In addition to the $\alpha$ and $\beta$ bands seen in the Fermi surface maps, the outermost $\gamma$ band is clearly observed. The sum of the LCP and RCP maps is displayed in Fig-

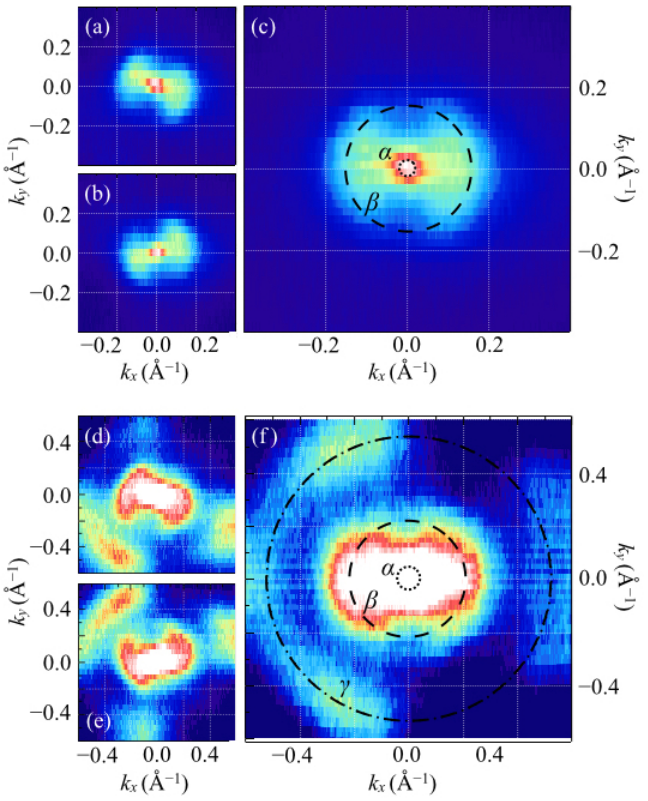


FIG. 1. (Color online) Fermi surface maps (integrated within ± 5 meV) with (a) left-handed circular polarization (LCP), (b) right-handed circular polarization (RCP), and (c) the sum of the LCP and RCP. The dotted and dashed circles roughly indicate the position of the $\alpha$ and $\beta$ Fermi surfaces. Photoemission intensity maps at 20 meV below $E_F$ (integrated within ± 5 meV) with (d) LCP, (e) RCP, and (f) the sum of the LCP and RCP. The photon energy for all the maps is fixed at 23 eV ($k_z$ = 2.97 Å$^{-1}$, which is near the Γ point). The dotted, dashed, and dot-dashed circles roughly indicate the position of the $\alpha$, $\beta$, and $\gamma$ bands.

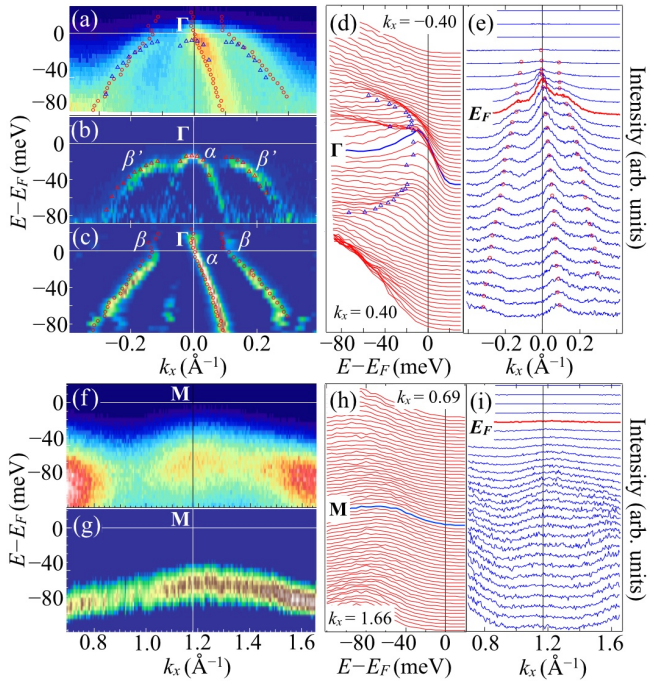


FIG. 2. (Color online) (a) Cuts around the Γ point along $k_x$, (b) curvature of EDCs, (c) curvature of MDCs (d) EDCs, and (e) MDCs. (f) Cuts around M point along $k_x$ , (g) curvature of EDCs, (h) EDCs, and (i) MDCs. The circles and triangles indicate the band positions obtained from the MDC and EDC, respectively.

ure 1(f) and the three hole bands are more clearly seen. The absence of $\gamma$ Fermi surface and the existence of $\gamma$ band at 20 meV suggests gap opening at $E_F$ in the $\gamma$ band.

Figures 2(a), (b), and (c) show the band dispersions along the cut around the Γ point as a function of $k_x$. Obtained from the energy distribution curves (EDCs) in Figure 2(d), the band dispersion labeled as $\beta'$ as well as from their curvatures [16] in Figure 2(b) does not reach $E_F$ and takes its maximum at the zone center. By contrast, the band dispersion of the $\beta$ band clearly crosses $E_F$, which is extracted from the momentum distribution curves (MDCs) in Figure 2(e). The same behavior can be seen in their curvatures in Figure 2(c).

This observation suggests that, in addition to the $\beta$ band forming the $\beta$ Fermi surface, another hole like band, which can be labeled as $\beta'$, exists around the zone center. Indeed, as shown in Figures 2(d) and (e), the intensity of the $\beta$ band drops for $|k_x|$ smaller than $\sim 0.175$ Å$^{-1}$ in the EDC and MDC plots, indicating that the $\beta$ band crosses $E_F$ at $|k_x| \sim 0.175$ Å$^{-1}$ which corresponds to the $\beta$ Fermi surface in Figure 1. On the other hand, some intensity remains even for $|k_x|$ smaller than $\sim 0.175$ Å$^{-1}$ and reaches the zone center, where this remaining band ($\beta'$) and the $\alpha$ band are almost degenerate.

Since the tops of the $\alpha$ and $\beta'$ band dispersions derived from the $yz/zx$ bands are almost degenerate at the zone center, the orbital degeneracy of $yz/zx$ remains at the zone center. The remaining $yz/zx$ orbital degeneracy may contradict with the most of the published results including a recent ARPES work by Miao *et al.* [17], that reported a ubiquitous $yz/zx$ splitting. On the other hand, this degeneracy is consistent with the ARPES work by Okazaki *et al.* [10]. In the present ARPES, the four hole bands ($\alpha$, $\beta$, $\beta'$, and $\gamma$) can be identified. Since only the three hole bands are expected near $E_F$ in the homogeneous FeSe or FeTe, the four hole bands indicate an electronic inhomogeneity to some extent. The four hole bands can be interpreted as the superposition of the two band structures with and without the degeneracy of the $yz/zx$ bands at the zone center. Namely, the system exhibits a sort of phase separation into the two electronic states with and without the electronic nematicity. The state with $\alpha$, $\beta$, and $\gamma$ bands is likely to be accompanied by the static or dynamic orthorhombic distortion for breaking the $yz/zx$ degeneracy. This state could be similar to the anisotropic or nematic state proposed by Miao *et al.* [17]. The other state with $\alpha$, $\beta'$, and $\gamma$ bands keeps the tetragonal symmetry with the $yz/zx$ degeneracy and corresponds to the non-nematic state. However, since the $\beta$ and $\beta'$ are not clearly separated, the energy splitting between the $yz$ and $zx$ bands should have distribution due to static inhomogeneity and/or dynamic fluctuation. That is to say, the nematic state and the non-nematic state coexist in the Ru substituted system.

Without the Ru substitution, the $\beta'$ band is not clearly observed under the same experimental condition [7]. In addition, the intensity and energy of the $\alpha$ band is strongly modified from the prediction of the band-structure calculation. In $FeSe_{1-x}Te_x$, the $\alpha$ band is located well below $E_F$ and is very broad even at the zone center. Therefore, Sudayama *et al.* assigned the modified $\alpha$ band to the $xy$ band from the FeSe-like orbital state [7]. This position of the $xy$ band is actually consistent with the recent ARPES study on FeSe [18], partially supporting the interpretation, i.e., it is possible that the $yz/zx$ orbital degeneracy is broken due to the participation of the $xy$ orbital in $FeSe_{1-x}Te_x$. On the other hand, the present results on the Ru substituted system indicate that the modified $\alpha$ band in $FeSe_{1-x}Te_x$ becomes normal (viz, comes close to the prediction of the band-structure calculation for the average structure) and the $\beta'$ band appears just below $E_F$. Consequently, the $yz/zx$ degeneracy ($\alpha$ and $\beta'$) at the zone center is recovered with the Ru substitution. Interestingly, such behavior is observed in as-grown $FeSe_{1-x}Te_x$ without annealing treatment [10, 19], suggesting that the static inhomogeneity is introduced by the Ru substitution or by the atomic disorder and the $yz/zx$ orbital degeneracy is partially recovered.

The band dispersions as functions of $k_x$ around the zone corner are displayed in Figures 2(f) and (g), and

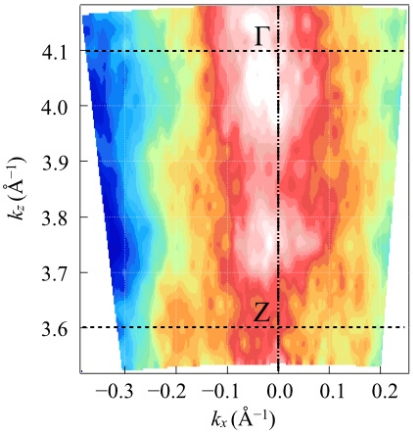


FIG. 3. (Color online) Fermi surface map in the $k_x$-$k_z$ plane. The ARPES spectra are integrated within ± 18 meV relative to $E_F$.

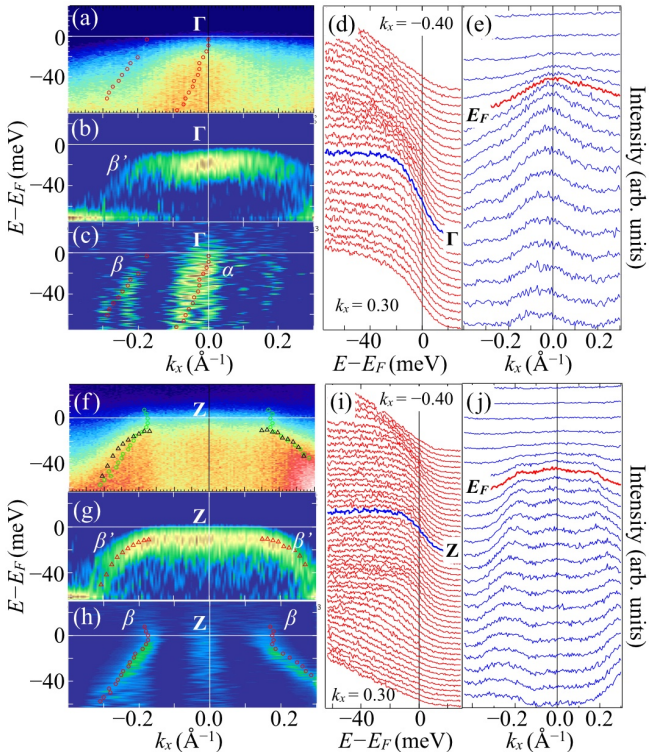


FIG. 4. (Color online) (a) Cuts around Γ point along $k_x$, (b) curvature of EDCs, (c) curvature of MDCs, (d) EDCs, and (e) MDCs. (f) Cuts around Z point along $k_x$, (g) curvature of EDCs, (h) curvature of MDCs, (i) EDCs, and (j) MDCs. The circles and triangles indicate the band positions obtained from the MDC and EDC, respectively.

the corresponding EDCs and MDCs are plotted in Figures 2(h) and (i). The EDC and MDC plots show that the spectral features are very broad near the zone corner compared to those of annealed $FeSe_{1-x}Te_x$ [7]. On the other hand, the spectral features near the zone center are comparable to those of $FeSe_{1-x}Te_x$. The similar momentum dependent broadening is observed in as-grown $FeSe_{1-x}Te_x$ without annealing treatment [19]. Such momentum dependent broadening suggests that the Ru substitution can introduce additional atomic disorder which can freeze the orbital/lattice fluctuations and reduce the $yz/zx$ splitting.

Figure 3 shows a Fermi surface map in the $k_x$-$k_z$ plane taken at $h\nu$ = 37 to 56 eV, showing good two-dimensionality of the $\beta$ Fermi surface although the intersection of the $\beta$ Fermi surface slightly increases in going from Γ ($k_z = 0$) to Z ($k_z = \pi/c$). The band-structure calculations with the average structure predict $k_z$ dependence of the Fermi surfaces and the $yz/zx$ splitting. For example, the doubly degenerate $yz/zx$ bands are located below the $xy$ band at Γ while they are located above the $xy$ band at Z in the calculations [6, 20, 21]. The increase of the $\beta$ Fermi surface area with $k_z$ is in qualitative agreement with the calculations. However, the area of the $\gamma$ Fermi surface is much larger than the calculations. The disagreement between the ARPES results and the calculations can be assigned to the moderate correlation effect and the random distribution of Se and Te, that can strongly disturb the momentum dependent interlayer coupling and provide the good two dimensionality to the Fermi surfaces.

In Figure 4, the band dispersions, EDCs and MDCs around the Γ and Z points of Figure 3 are displayed. The band dispersions around Γ are more or less consistent with those in Figure 2. The $\alpha$, $\beta$, and $\beta'$ bands can be identified since the intensity of the $\beta/\beta'$ band drops for $|k_x|$ smaller than $\sim 0.175$ Å$^{-1}$ but some intensity remains even for $|k_x|$ smaller than $\sim 0.175$ Å$^{-1}$ and reaches the zone center. Again, this is consistent with the picture of the strong lattice disorder and the coexistence of the nematic and non-nematic electronic states.

In summary, the multi-band electronic structure of the Ru substituted $FeSe_{1-x}Te_x$ has been studied by means of ARPES. With the Ru substitution, the $\gamma$ Fermi surface with the Fe 3$d$ $xy$ character is suppressed and the band dispersions near the zone boundaries are broadened. These observations indicate strong lattice disorder introduced by the Ru substitution. While the degeneracy of the Fe 3$d$ $yz/zx$ bands at the zone center is broken in $FeSe_{1-x}Te_x$, it is partly recovered in the Ru substituted $FeSe_{1-x}Te_x$. This behavior is further confirmed by the $k_z$ dependent ARPES measurements and shows that the strong lattice disorder by the Ru substitution causes the coexistence of the nematic and non-nematic electronic states. The moderate electronic correlation effect and the random distribution of Se and Te, which would play essential roles for the electronic nematicity in $FeSe_{1-x}Te_x$, are disturbed by the Ru substitution.

This work was partially supported by Grants-in-Aid from the Japan Society of the Promotion of Science (JSPS) (Grant No: 25400356). T.S. and D.O. acknowl-

edge supports from the JSPS Research Fellowship for Young Scientists. The synchrotron radiation experiments have been done with the approval of Photon Factory, KEK (2013G021) and Hiroshima Synchrotron Radiation Center (Proposal No.13-A-6).

[1] Y. Kamihara, T. Watanabe, M. Hirano, and H. Hosono, J. Am. Chem. Soc. **130**, 3296 (2008).
[2] F. C. Hsu, J. Y. Luo, K. W. The, T. K. Chen, T. W. Huang, P. M. Wu, Y. C., Lee, Y. L. Huang, Y. Y. Chu, D. C. Yan, M. K. Wu, Proc. Natl. Acad. Sci. U.S.A. **105**, 14262 (2008).
[3] T. M. McQueen, A. J. Williams, P. W. Stephens, J. Tao, Y. Zhu, V. Ksenofontov, F. Casper, C. Felser, and R. J. Cava, Phys. Rev. Lett. **103**, 057002 (2009).
[4] W. Bao, Y. Qiu, Q. Huang, M. A. Green, P. Zajdel, M. R. Fitzsimmons, M. Zhernenkov, S. Chang, M. Fang, B. Qian, E. K. Vehstedt, J. Yang, H. M. Pham, L. Spinu, Z. Q. Mao, Phys. Rev. Lett. **102**, 247001 (2009).
[5] T. Noji, T. Suzuki, H. Abe, T. Adachi, M. Kato, Y. Koike, J. Phys.Soc. Jpn. **79**, 084711 (2010).
[6] F. Chen, B. Zhou, Y. Zhang, J. Wei, H. W. Ou, J. F. Zhao, C. He, Q. Q. Ge, M. Arita, K. Shimada, H. Namatame, M. Taniguchi, Z. Y. Lu, J. P. Hu, X. Y. Cui, and D. L. Feng, Phys. Rev. B **81**, 014526 (2010).
[7] T. Sudayama, D. Ootsuki, Y. Wakisaka, T. Mizokawa, N. L. Saini, M. Arita, H. Namatame, M. Taniguchi, T. Noji, and Y. Koike, J. Phys. Soc. Jpn. **82**, 053705 (2013).
[8] K. Nakayama, T. Sato, P. Richard, T. Kawahara, Y. Sekiba, T. Qian, G. F. Chen, J. L. Luo, N. L. Wang, H. Ding, T. Takahashi, Phys. Rev. Lett. **105**, 197001 (2010).
[9] A. Tamai, A. Y. Ganin, E. Rozbicki, J. Bacsa, W. Meevasana, P. D. C. King, M. Caffio, R. Schaub, S. Margadonna, K. Prassides, M. J. Rosseinsky, F. Baumberger, Phys. Rev. Lett. **104**, 097002 (2010).
[10] K. Okazaki, Y. Ito, Y. Ota, Y. Kotani, T. Shimojima, T. Kiss, S. Watanabe, C.-T. Chen, S. Niitaka, T. Hanaguri, H. Takagi, A. Chainani, and S. Shin, Sci. Rep. **4**, 109 (2013).
[11] B. Joseph, A. Iadecola, A. Puri, L. Simonelli, Y. Mizuguchi, Y. Takano, N. L. Saini, Phys. Rev. B **82**, 020502 (2010).
[12] M. Nakajima, T. Lianga, S. Ishida, Y. Tomioka, K. Kihou, C. H. Lee, A. Iyo, H. Eisaki, T. Kakeshita, T. Itob, and S. Uchida, Proc. Natl. Acad. Sci. U.S.A. **108**, 12238 (2011).
[13] S. Ishida, M. Nakajima, T. Liang, K. Kihou, C.-H. Lee, A. Iyo, H. Eisaki, T. Kakeshita, Y. Tomioka, T. Ito, S. Uchida, J. Am. Chem. Soc. **135**, 3158 (2013).
[14] M. N. Gastiasoro, P. J. Hirschfeld, and B. M. Andersen, Phys. Rev. B **89**, 100502 (2014).
[15] T. Inabe, T. Kawamata, T. Noji, T. Adachi, Y. Koike, J. Phys. Soc. Jpn. **82**, 044712 (2013).
[16] P. Zhang, P. Richard, T. Qian, Y.-M. Xu, X. Dai, and H. Ding, Rev. Sci. Instrum. **82**, 043712 (2011)
[17] H. Miao, L.-M. Wang, P. Richard, S.-F. Wu, J. Ma, T. Qian, L.-Y. Xing, X.-C. Wang, C.-Q. Jin, C.-P. Chou, Z. Wang, W. Ku, and H. Ding, Phys. Rev. B **89**, 220503 (2014).
[18] J. Maletz, V. B. Zabolotnyy, D. V. Evtushinsky, S. Thirupathaiah, A. U. B. Wolter, L. Harnagea, A. N.Yaresko, A. N. Vasiliev, D. A. Chareev, A. E. Böhmer, F. Hardy, T. Wolf, C. Meingast, E. D. L. Rienks, B. Büchner, and S. V. Borisenko, Phys. Rev. B **89**, 220506 (2014).
[19] T. Sudayama, Y. Wakisaka, D. Ootsuki, M. Arita, H. Namatame, M. Taniguchi, T. Noji, Y. Koike, N. L. Saini, and T. Mizokawa, unpublished.
[20] A. Subedi, L. Zhang, D. J. Singh, and M. H. Du, Phys. Rev. B **78**, 134514 (2008).
[21] T. Miyake, K. Nakamura, R. Arita, and M. Imada, J. Phys. Soc. Jpn. **79**, 044705 (2010).